

Photonic crystal fiber design for broadband directional coupling

Jesper Lægsgaard, Ole Bang, and Anders Bjarklev

Research Center COM, Technical University of Denmark, Building 345v, DK-2800 Kongens Lyngby, Denmark

Received July 14, 2004

A novel design for a broadband directional coupler based on a photonic crystal fiber is investigated numerically. It is shown that suitable index-depressing doping of the core regions in an index-guiding twin-core photonic crystal fiber can stabilize the coupling coefficient between the cores over an extremely broad (octave-spanning) frequency range. © 2004 Optical Society of America

OCIS codes: 060.1810, 060.2280, 060.2340.

Photonic crystal fibers (PCFs), which guide light by coherent scattering from an array of micrometer-sized airholes running along the fiber axis, offer remarkable flexibility in the design of fiber structure and waveguiding properties compared with conventional optical fibers.¹ Much activity has in recent years been directed toward utilizing this flexibility to engineer properties such as group-velocity dispersion,^{2,3} mode area,⁴ and numerical aperture⁵ in single-core fibers, and it has been demonstrated that these quantities can be pushed into parameter ranges that are inaccessible to traditional fiber technology. Recently, several groups of scientists investigated PCF-based directional couplers, manufactured directly as a twin-core PCF,^{6,7} by the fused biconical tapered method,⁸ or by joining two side-polished single-core PCFs.⁹ Therefore it is of interest to investigate the potential of PCFs for improving the properties of directional couplers. In particular, an increase in bandwidth compared with those of current fiber couplers would be important for a number of applications, including telecommunication networks and fiber-based optical coherence tomography systems.

With respect to broadband directional coupling, an interesting idea was put forward by Mangan *et al.*¹⁰ They demonstrated experimentally that a silica-air PCF with its core index depressed by fluorine doping exhibits a guided mode whose mode field area initially contracts with decreasing wavelength but at a certain threshold begins to expand again until a short-wavelength cutoff for mode guidance is reached. The reason for this behavior is the fact that the effective index of the microstructured silica-air cladding is strongly wavelength dependent and tends toward the refractive index of pure silica within the short-wavelength limit.¹¹ Therefore at a certain threshold wavelength the effective cladding index exceeds the index of the doped core, which then ceases to support a guided mode. In relation to directional fiber couplers, the existence of a minimum in the mode area is interesting because one can expect, by the same reasoning, that the coupling length of a twin-core PCF with depressed-index cores will show a maximum at some wavelength. At this wavelength, then, the twin-core PCF may form the basis of an unusually broadband

directional coupler because of the vanishing first derivative of the coupling length.

Here we numerically investigate the wavelength variation of the coupling length in a twin-core PCF structure with depressed-index cores. We show that the proper choice of the radius and the index contrast of the doped regions can lead to stabilization of the coupling length over extreme wavelength intervals spanning an octave or more. Thus this type of fiber coupler has the potential to remove completely the bandwidth limitations that arise from directional couplers in most optical systems.

The generic design that we investigate is shown schematically in Fig. 1. We formed a twin-core structure in a perfect hexagonal array of airholes in silica by removing two airholes separated by two lattice units. In each core the refractive index within a radius of $d_c/2$ was decreased by doping. Thus the defining parameters of the structure are the hole diameter d , the lattice constant (commonly denoted the pitch) Λ , the absolute refractive-index difference between pure and doped silica regions Δ , and the diameter of

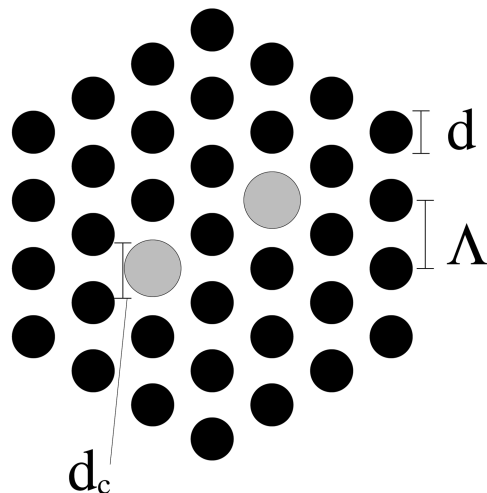


Fig. 1. Generic PCF design studied here. Darker circles represent airholes; lighter circles indicate possibly doped regions in the core regions. Only the airhole rings closest to the core region are shown. For all the calculations reported we used $d/\Lambda = 0.5$.

these regions d_c . As the Maxwell equations are scale invariant, we measured all other lengths in units of Λ . The results found may then be scaled to any physical pitch value.

Of course, there are many other ways of forming a twin-core structure in a hexagonal airhole array than the one shown in Fig. 1. However, it is our purpose in this Letter not to investigate different twin-core designs but rather to elucidate how the design of the doped core influences the coupling coefficient. For this purpose, a detailed analysis of the structure in Fig. 1 suffices.

We obtained the PCF eigenmodes by expanding the magnetic field and the PCF dielectric function in plane waves using a freely available software package.¹² All the results shown were obtained for a value of $d/\Lambda = 0.5$ for the relative airhole diameter. The refractive index of pure silica was taken to be 1.45, and dispersion of both pure and doped silica was neglected. In a real fiber, dispersion effects may slightly change the quantitative results obtained but are not expected to affect the overall conclusions. Because of inversion symmetry, two guided-mode eigenstates are found for each polarization direction: one that is even with respect to inversions about the airhole separating the two cores and one that is odd. Coupling length L_c of the directional coupler at a given frequency is determined from the difference in propagation constants of the even and the odd modes:

$$L_c^\sigma = \frac{\pi}{\beta_e^\sigma - \beta_o^\sigma}, \quad (1)$$

where β_o^σ and β_e^σ are the propagation constants of odd and even modes, respectively, and σ is a polarization-state index. The twin-core structure is slightly birefringent, and, as it turns out, the polarization state direction that has the highest value of β_e has the lowest value of β_o . Therefore a substantial difference (approximately 2–5% in the region of interest) in coupling length arises between the two polarization directions. For simplicity we give results only for the polarization direction parallel to the direction between the two cores, which has the shortest coupling lengths; the polarization index on L_c is suppressed. However, similar conclusions are obtained when the other polarization direction is considered. We can probably reduce the polarization dependence of L_c by changing the relative positions of the two cores in the airhole matrix.

All the calculations reported here were performed in a rectangular supercell of dimensions $8\Lambda \times 5\sqrt{3}\Lambda$, where Λ is the center-to-center distance between neighboring airholes, as depicted in Fig. 1. A Fourier grid of 784×845 points was used. Convergence checks indicated that these parameters ensure convergence of the coupling lengths to a level of approximately 1%. Convergence with respect to supercell size was enhanced by use of the coupling-reducing transverse \mathbf{k} point (0.25, 0.25).¹³

In Fig. 2, coupling lengths L_c for four generic-type fiber designs depicted in Fig. 1 are shown as a function of normalized frequency. The parameters that define

the doped core region are indicated in Fig. 2. It is evident that, whereas the undoped twin-core structure shows a monotonic increase of L_c with frequency, the doped fibers display a maximum value of L_c . However, the behavior of the L_c curve is critically dependent on core design. For a large radius of the doped region, the maximum occurs at a relatively low frequency, and shortly thereafter the fiber ceases to support guided modes. However, if the radius of the doped region is decreased, the maximum is broadened considerably, and the short-wavelength cutoff for mode guidance moves up in frequency, even though the magnitude of the doping-induced index contrast Δ increases correspondingly. Eventually the fiber enters a regime where L_c displays first a local maximum and then a local minimum at a shorter wavelength, after which it continues to grow with frequency. It is evident that the L_c curve in this regime can be made extraordinarily flat by choice of a value of d_c that is comparable with the diameter of the airholes, as illustrated by the long-dashed curve in Fig. 2.

This important finding may be rationalized as follows: The strong wavelength dependence of the effective cladding index comes about because the light at short wavelengths avoids the cladding airholes more efficiently. Mode guidance is cut off when the effective cladding index exceeds the index of the doped core. However, when the doping radius is reduced, a similar effect is at work in the core itself: At short wavelengths the light more easily avoids the doped region, so the effective index of the core increases. This increase broadens the maximum of the L_c curve and pushes the guided-mode cutoff to shorter wavelengths until it eventually disappears.

To illustrate the potential of the fiber with $\Delta = 0.004$ and $d_c/\Lambda = 0.46$ we show a practical design example in Fig. 3: The pitch of the fiber was chosen to be $\Lambda = 12 \mu\text{m}$ to produce a flat L_c function spanning the vacuum wavelength interval of 750–1500 nm. Of course, this wavelength range could be shifted by another choice of Λ . The length of coupling device L_d was taken to be half of the value of the midpoint

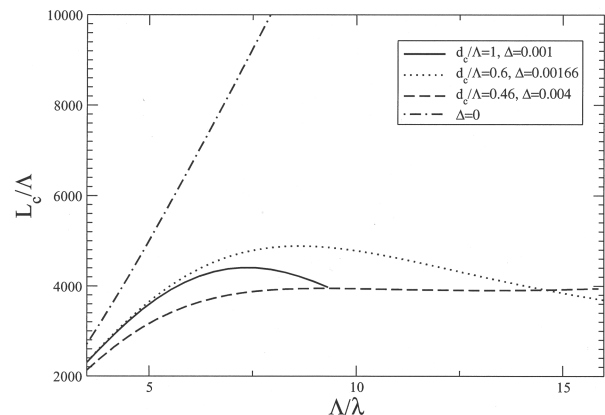


Fig. 2. Coupling length L_c relative to pitch Λ as a function of normalized frequency Λ/λ for four twin-core fibers. Δ denotes the index contrast between the base material and the index-depressed core regions, whereas d_c denotes the diameter of these regions.

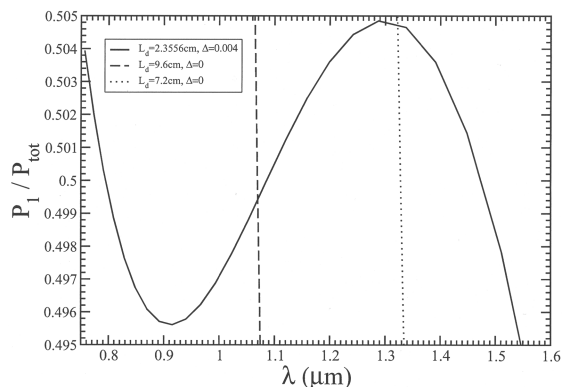


Fig. 3. Power fraction P_1/P in the launch arm at the output end of a fiber coupler based on the twin-core photonic crystal fiber structure in Fig. 1 with $\Lambda = 12 \mu\text{m}$, $d_c = 5.52 \mu\text{m}$, device length L_d , and index step between doped and undoped regions Δ .

between the local maximum and the local minimum of the L_c curve. The fraction of power in the launch arm of the coupler at the output port was determined to be $P_1/P_{\text{tot}} = \cos^2(\pi L_d/2L_c)$. It can be seen that the value of P_1/P_{tot} is stabilized at 0.495–0.505 over a wavelength interval of slightly more than an octave. For comparison, two curves calculated with an undoped twin-core structure that has the same value of Λ but two values of L_d are also shown. The coupling ratio of these devices passes through the reported range over a wavelength interval of ~ 10 nm, a behavior that is quite similar to that of directional couplers based on standard optical fibers or planar waveguides and clearly demonstrates that it is the index depression of the core that is decisive in stabilizing the coupling ratio as a function of frequency.

In conclusion, it has been demonstrated that the bandwidth of a fiber-based directional coupler can be strongly enhanced by the use of a twin-core photonic

crystal fiber that has regions of depressed index in the cores. By proper choice of radius and index contrast of the doped regions it is possible to stabilize the coupling ratio over extreme wavelength intervals that span an octave or more.

J. Lægsgaard (jl@com.dtu.dk) is financially supported by the Danish Technical Research Council.

References

1. A. Bjarklev, J. Broeng, and A. S. Bjarklev, *Photonic Crystal Fibres* (Kluwer Academic, Dordrecht, The Netherlands, 2003).
2. F. Poli, A. Cucinotta, M. Fuochi, S. Selleri, and L. Vincetti, *J. Opt. Soc. Am. A* **20**, 1958 (2003).
3. N. I. Nikolov, T. Sorensen, O. Bang, and A. Bjarklev, *J. Opt. Soc. Am. B* **20**, 2329 (2003).
4. T. M. Monro, D. J. Richardson, N. G. R. Broderick, and P. J. Bennett, *J. Lightwave Technol.* **17**, 1093 (1999).
5. K. Furusawa, A. Malinowski, J. H. V. Price, T. M. Monro, J. K. Sahu, J. Nilsson, and D. J. Richardson, *Opt. Express* **9**, 714 (2001), <http://www.opticsexpress.org>.
6. B. J. Mangan, J. C. Knight, T. A. Birks, P. St. J. Russell, and A. H. Greenaway, *Electron. Lett.* **36**, 1358 (2000).
7. W. E. P. Padden, M. A. van Eijkelenborg, A. Argyros, and N. A. Issa, *Appl. Phys. Lett.* **84**, 1689 (2004).
8. B. H. Lee, J. B. Eom, J. Kim, D. S. Moon, U.-C. Paek, and G.-H. Yang, *Opt. Lett.* **27**, 812 (2002).
9. H. Kim, J. Kim, U.-C. Paek, and B. H. Lee, *Opt. Lett.* **29**, 1194 (2004).
10. B. J. Mangan, J. Arriaga, T. A. Birks, J. C. Knight, and P. St. J. Russell, *Opt. Lett.* **26**, 1469 (2001).
11. T. A. Birks, J. C. Knight, and P. St. J. Russell, *Opt. Lett.* **22**, 961 (1997).
12. S. G. Johnson and J. D. Joannopoulos, *Opt. Express* **8**, 173 (2001), <http://www.opticsexpress.org>.
13. M. Albertsen, J. Lægsgaard, S. E. B. Libori, K. Hougaard, J. Riishede, and A. Bjarklev, *Photon. Nanostruct.* **1**, 43 (2003).